25th ABCM International Congress of Mechanical Engineering
October 20-25, 2019, Uberlândia, MG, Brazil

COB-2019-0199
NUMERICAL AND EXPERIMENTAL DEVELOPMENT OF THE WING STRUCTURE OF A HUMAN-POWERED AIRCRAFT (HPA)

Marcelo Otávio dos Santos
Joseph Youssif Saab Junior
Caroline Colaço Spina
Luciano Neres Correia Paes
Matheus Gomes do Amaral
Instituto Mauá de Tecnologia (IMT) - Centro Universitário Mauá – Campus- São Caetano do Sul - Praça Mauá 1 - 09580 900 - São Caetano do Sul – SP - Brazil.
marcelo.santos@maua.br
saab@maua.br
caroline.c.spina@gmail.com
lucianopaes92@gmail.com
matheusgomes205@gmail.com

Abstract. *The objectives of the present work were to design, simulate, construct and validate the structural components of the wing of a human-powered aircraft (HPA), the "Tuiuiu", an academic project undergoing development at the Instituto Mauá de Tecnologia (IMT). After definition of the flight requirements, initial sizing of the empty and total weights, wing area and estimation of the human power available as a function of time, the detailed aerodynamic design was started and generated the V-n chart and the corresponding aerodynamic loads for the design of the most important structural member of the HPA: the wing-spar. The aerodynamic loading derived from the flight conditions were first assessed via a hybrid, Euler-integral solver (XFLR5), and later refined by finite volume (ANSYS CFD) resolution of the fluid movement equations around the wing geometry. With the final and ultimate loads figures and distribution along the span , it was possible to relate shapes, stiffness and density of various materials in order to determine what would be the ideal design of the wing spar as well as the most suitable material for its manufacture. The component parts of the wing were modeled in the NX CAD software and then exported for a finite element method (FEM) simulation (ANSYS Mechanical). Structural optimizations were made to adapt the characteristics of the wing to the constraints of the project. Finally, two prototypes were manufactured where strength and structural stiffness validation analyzes were performed. Differences of 2.8% and 7.3% in stress and deformation, respectively, were obtained among the reference experimental values and the numerical results.*

Keywords: *Human Powered Aircraft (HPA). Light aircraft spar sizing. CAE simulation. Composite material FEM simulation.*

1. INTRODUCTION

Until 1959, no aircraft had been able to fly powered by human propulsion alone, prompting industrialist Henry Kremer to offer a prize for the first aircraft to make a flight traced around two poles set apart by at least 802 meters . Further the aircraft should fly over two 3-m high obstacles immediatelly after take-off and before landing and would have to take off and fly on human power, only(Royal Aeronautical Society, 2017). The original prize of £ 5,000 offered in 1959 was increased to £ 50,000 in 1973 and remained with no successful[1] claim until it was won on August, 1977, by a team led by the late Dr Paul MacCready Jr, the pilot Bryan Allen and the Gossamer Condor crew (Burke, 1980). After that, other HPAs were successfully developed, notably the Channel crossing by the Gossamer Albatross, the 115-km Crete-Santorini flight by the Daedalus, and also the Velair 89 and Musculair, which fle in Germany with outstanding performances. Although some of the described designs were supported by resources from companies, experienced engineers and graduate students, at the Instituto Mauá de Tecnologia, the "Tuiuiu" HPA project was proposed as an interdisciplinary, project-based learning (PBL) subject and is being developed solely by undergraduate students, which get acquainted with the project and advance a small part of it each term. This paper reports the design, simulation and experimental validation of the wing spar of the HPA - Tuiuiu wich is being developed under a challenging context at the Instituto Mauá de Tecnologia.

[1] The SUMPAC, from graduated students of the Southampton University flew in 1961, but failed to complete the "Figure of 8" Kremer prize requirements.

1.1 Aerodynamics

When a body moves through a fluid, the integration of the local tangential and normal forces along the body surface return an aerodynamic resultant force that, for analysis reasons, may be projected in the direction of the flight, which is caled the lift force (L), and in the direction perpendicular do the flight, which is called the drag force (D). If the aerodynamic resultant force is not applied to the center of pressure of the boby, a moment will also arise in order to represent the fluid-body interaction complely as can be seen in Figure 1. These aerodynamic forces depend on the the wing reference aera (S), usually a normal projection of the wing area in flight condition; on velocity of the plane (V) and on the air density (ρ). The aerodynamic forces and moments are most often represented by their respective dimensionless coeficients, the lift coefficient (C_L) , the drag coefficient (C_D) and the moment coefficient (C_M), whose measuring point must be specified and is usually at 25% of the mean aerodynamic chord of the wing.

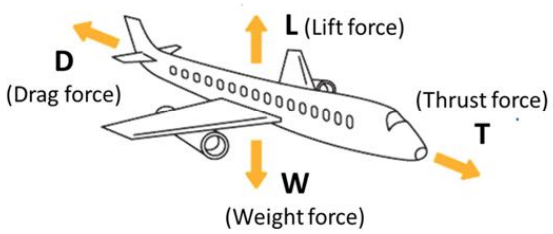

Figure 1. Forces acting on an airplane during a straight flight with constant speed.

Besides the lift and drag forces, others forces acting on the plane during the flight such as the weight (W) and thrust (T) must be specified in order to determine completely the dynamics of flight, which is only sustainable if the lift and thrust forces are greater than the drag and the aircraft's weight forces, respectively. It is well know nowadays that sutained and maneuvrable flight is only possible when the fundamental and interdependent set of ratios called the wing loading (W/S), which is the aircraft weight-to-wing-area ratio; the specific power (T/W), wich represents the aircraft thrust to nd weight; and the aerodynamic efficiency (C_L/C_D), which is the ratio of lift coefficient (C_L) to the drag coefficient (C_D), are set correctly for the design and mission of the airplane (Anderson Jr., 1999) (Torenbeek, 2013).

2. DEVELOPMENT

2.1 HPA Configuration and Material Selection

In order to determine the configuration of the aircraft to be designed, previous parameters and configurations of HPAs that succeeded in their missions were used. First of all, aircraft models that were able to fly were selected, and then only the aircraft models that were able to reach the speed of 10m/s, the minimum average speed to qualify for the newest Kermer HPAS set of requirements, were filtered. Those aircrafts were used as references while sizing the fundamental flight parameters, such as the wing loading, specific power and aerodynamic efficiency.

In order to determine the material of the wing spar, optimization and structural performance calculations were accomplished based on the case study on Ashby (2010). It was taken into account that the design criteria would be (i) the maximum deflection and (ii) the allowable stresses at the spar structure. A further requirement introduced was that the wing flexure should be limited to a maximum of 600mm at the tips, based on the proposal of Sóbester & Foster (2015), so that no significant loss of lift would be experimented due to reduction of the projected wing area due to flexion under flight loads.

The shape factors for bending and torsional stiffness were calculated using Eq. (1) to (3).

$$\Phi_B^e = \frac{12l}{A^2} \tag{1}$$

$$\Phi_T^e = 7{,}14\frac{K}{A^2} \tag{2}$$

$$M = \frac{(\Phi_B^e E)^{\frac{1}{2}}}{\rho} \tag{3}$$

The wing spar cross-section was defined as circular and it would be manufactured from carbon-fiber-reinforced epoxy polymer, so that the physical and mechanical properties would be similar to those of the *Epoxy + 79% - T800 composite* from Niu (2001).

2.2 Definition of flight loads

The aerodynamic simulation software used for determing the lift distribution along the span was the XFLR5 (Drela, Youngren, & Deperrois, 2009), which is an open source hybrid code that matches the inviscid flow away from the airfoil with an integral formulation of the viscous boundary-layer at the displacement thickness line. Both fields are solved simultanously via the Newton method and the velocity and pressure fields are consistently returned for angles of attack bellow the stall angle (Drela & Giles, 1987). The far field (lift force) prediction of the XLFR5 is reliable and consistent, provided the angle of attack is kept below the stall angle. However, the 3D drag estimation of the code is not reliable and was supplemented by CFD calculations of the geometric drag employing the ANSYS CFX® code. Fortunatelly, the wing moment of inertia is usually very high for stresses applied in the chord plane, such as the drag force, and also, for a wing, the drag force is at least one order of magnitude lower than the lift force, so that the lift loading distribution only was considered while sizing the tubular wing spar. Based on the XFOIL reliable far-field calculation of the lift distribution, it was possible to simulate diferent types of airfoils in order to select the one with the suitable performance (with large values of C_L/C_D and ${C_L}^{3/2}/C_D$ ratios) and then simulate the 3D wing with the selected PF25 airfoil in order to determine the cruise angle of attack which allowed a straight, level flight, also referred to as a 1 G flight.

The wing was divided into several sections with a step of 0.2245m in order to determine the lift (C_L), drag (C_D) and moment (C_M) coefficients for each section, while varying the angle of attack (AoA) between +6° and -6°, safely within the non-stalled regime of the airfoil at the typical Reynolds number of 700,000, characteristic of the incompressible flow of small-velocity HPA flight. After the aerodynamic simulations were completed, it was concluded that for the PF25 airfoil, the higher aerodynamic efficiency of the wing was achieved for an A_OA of 1.1°.

Next, the C_L was calculated for the cruising condition, where the lift force is equal to the weight of the aircraft and the result was an lift coefficient of 0,94 for an attack angle of 1,1°. With this angle, it was possible to calculate the lift force distribution in each section of the wing, wich was divided in 0.2245m sections for the XFLR5 3D calculation.

With the determination of the 1 G reference flight load, the distribution was multiplied by the positive maneuver coefficien, n, which was selected as 1.31 in order to allow maximum banking of 40° during turns, resulting in the Final Load of the design. The Final Load was further multiplied by a safety factor of 2.0 so as to obtain the Ultimate Load. Both loads distribution along the wingspan with and without the correction coefficients may be seen in Fig. 2.

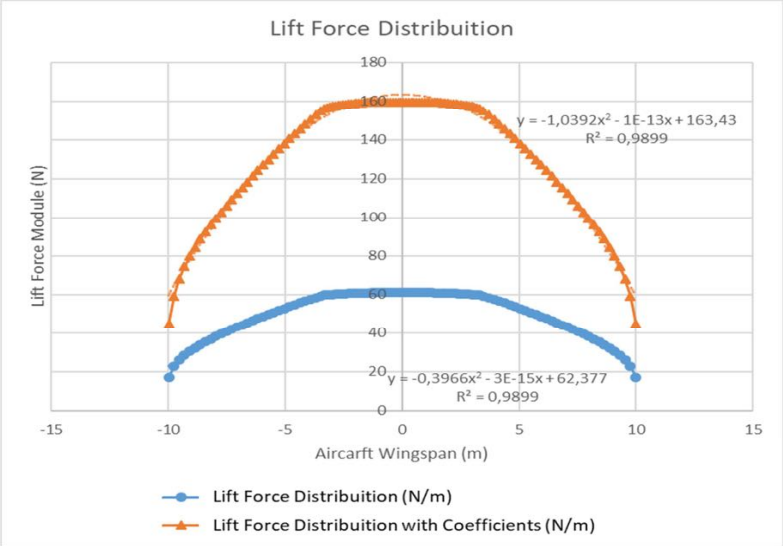

Figure 2. Load distribution along the wingspan with and without correction coefficients.

2.3 Numerical Simulation and Optimization

The material adopted for the wing spar during FEM simulation was Epoxy composite with carbon fiber (230 GPa) PrePreg, whose composition was 50% Pyrofil® TR 30S 3L twill 2x2/50% Epoxy resin and whose mechanical properties can be seen in Table 1.

Table 1. Mechanical properties of the Epoxy composite

Density	Shear Stress	Longitudinal Tension Stress	Longitudinal Compression Stress
1,420 kg/m³	125 MPa	805 MPa	509 MPa

Due to the wing symmetry, the optimization process and numerical simulations were done considering only half of the spar. So, as the whole spar has 20,200mm, it was considered 10,100mm for the total lengh during the numerical simulation phases. The first version, called Version 1, of the half wing spar was divided in two parts, called Section 1 and 2, with tubular transversal sections from different diameters. The outer diameter (*D*), the thickness (*t*) and the lengh (*L*) from each section are represented in Fig. 3, as its configuration.

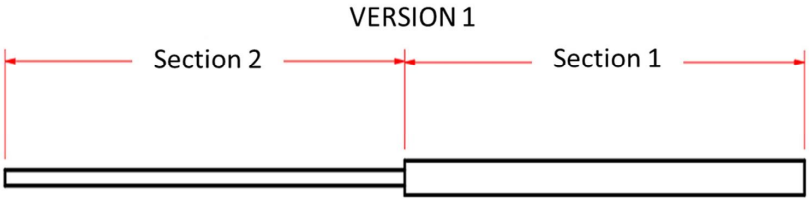

	Dimensions (mm)		
Section	D	t	L
1	76	4	4000
2	68	4	6100

Figure 3. Configuration and dimensions of half spar (Version 1).

The wing spar structure was discretized according to shell elements (2D), predominantly quadrilateral type of 8 nodes, totaling 11,373 elements. This structure version was 12.5kg weight and its deflection in the tip, wich can be seen in Fig. 4, was about 983mm, both above the stipulated limits of, respectively, 7kg and 600mm.

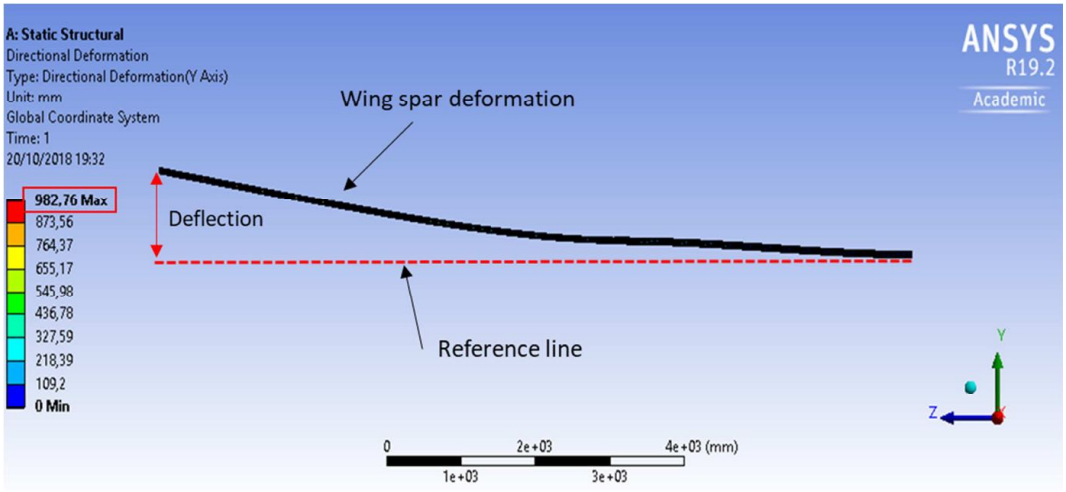

Figure 4. Wing spar deformation (Version 1).

In result of that, another configuration was stipulated. The second version, called Version 2, of the spar continued to have two parts, called Section 1 and 2, but with diferent dimensions, wich were based on the proportions of the HPA Daedalus wing spar. The study made by Vanderhoydonck (2016) showed that the spar diameter and the airfoil should vary linearly along the wing length. The external diameter of the spar root should be equal to 65% of the airfoil respective section height, and the external diameter of the free extreme (wing tip) should correspond to 80% of the airfoil respective section height.

Thus, the Version 2 dimensions and configuration are represented in Fig. 5. The section 2 is conical in shape with its external diameter ranging from 115mm (at junction with section 1) to 64mm at the free extreme.

	Dimensions (mm)		
Section	D	t	L
1	115	2	4000
2	115 64	2	6100

Figure 5. Configuration and dimensions of half spar (Version 2).

The Version 2 structure was also discretized according to shell elements (2D), predominantly quadrilateral type of 8 nodes, totaling 16,116 elements. This version os spar was 9.1kg weight and its deflection in the tip, wich can be seen in Fig. 6, was about 1,967mm.

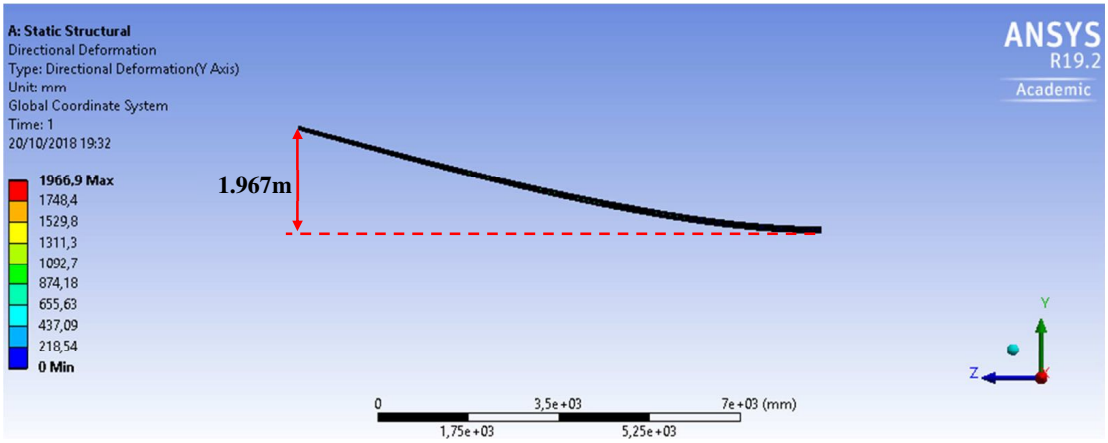

Figure 6. Wing spar deformation (Version 2).

Despite the mass decrease from 12.5kg to 9.1kg it was still above the limit, so the third configuration, called Version 3, was stipulated. To reach the dimensional requirements of the wing components, the half of the wing spar now was divided into 3 parts, called Section 1, 2 and 3, according to Fig. 7.

The sections 1 and 2 was designed with constant diameter and section 3 was designed with a variable diameter, but all tubular and whose dimensions have been defined based on a structural optimization study. The section 3 is conical in shape with its external diameter ranging from 110.2mm (at junction with section 2) to 64mm at the free end.

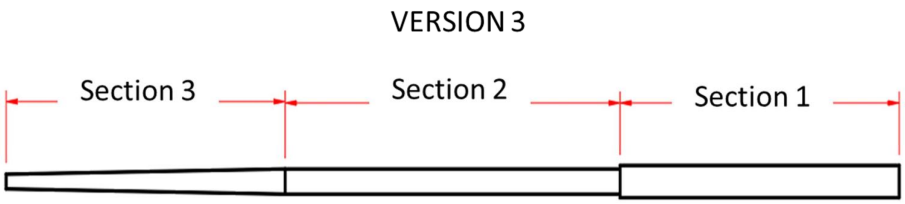

	Dimensions (mm)		
Section	D	t	L
1	115	1,2	3060
2	112,6	1,2	2380
3	110,2 64	1,2	4660

Figure 7. Configuration and dimensions of half spar (Version 3).

The wing spar geometry was prior modeled in NX CAD and then transferred to the simulation software ANSYS, where it was converted into surface element (Fig. 8).

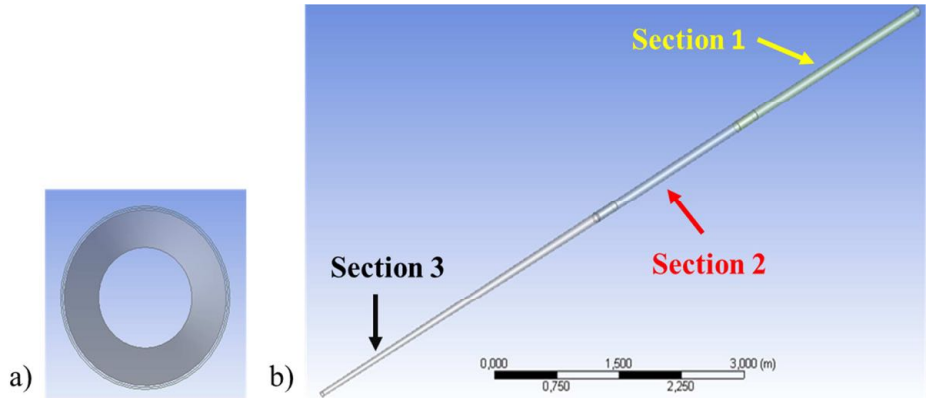

Figure 8. a) Front view of the wing spar (Version 3), b) proposed wing spar division (Version 3).

The Version 3 structure was also discretized with shell elements (2D). The mesh refinements were applied to the connections parts (between sections 1 and 2, 2 and 3) and the tip (section 3), in order to obtain more accurate results in the regions of higher stress gradients. In the connections, second order triangular elements of 5mm size were generated and in the tip of the spar (section 3), where the greatest deflection occurs, quadrilateral elements with 8 nodes were generated with the *face sizing* tool in order to standardize the mesh and obtain a more precise result. The size of the generated elements in section 3 was 10mm, totalizing about 38,200 triangular-type elements at the joints and 14,000 quadrilateral elements in section 3. In Figure 9 is possible to see the meshing in connections and section 3.

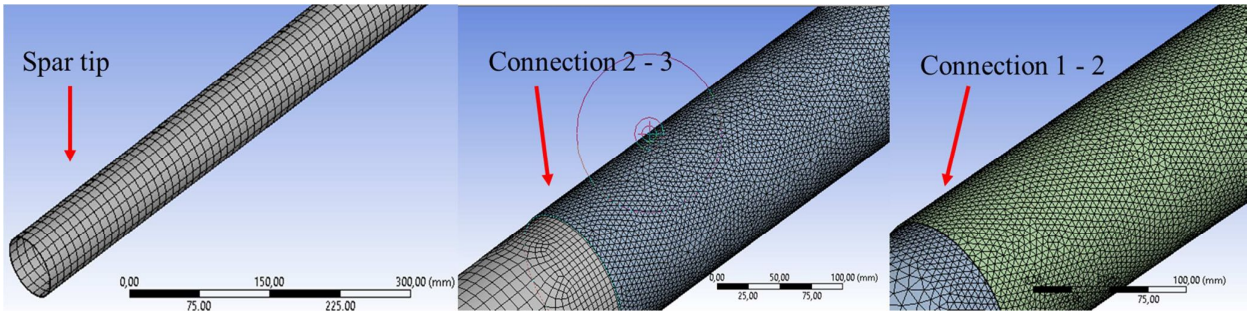

Figure 9. The generated mesh in the connections between sections 1-2 and 2-3 and in the spar tip.

The software ANSYS Composite Pre (ACP) was used to model the four composite layers of the Version 3 of wing spar, of wich the projected wing spar is composed. Each layer was 0.3mm thick and its fibers had different directions to better withstand the shear stress. The fibers of the layers 1 and 3 were directed in the axial direction of the wing spar while the layers 2 and 4 were oriented at -45° and 45°, respectively, according to Fig. 10.

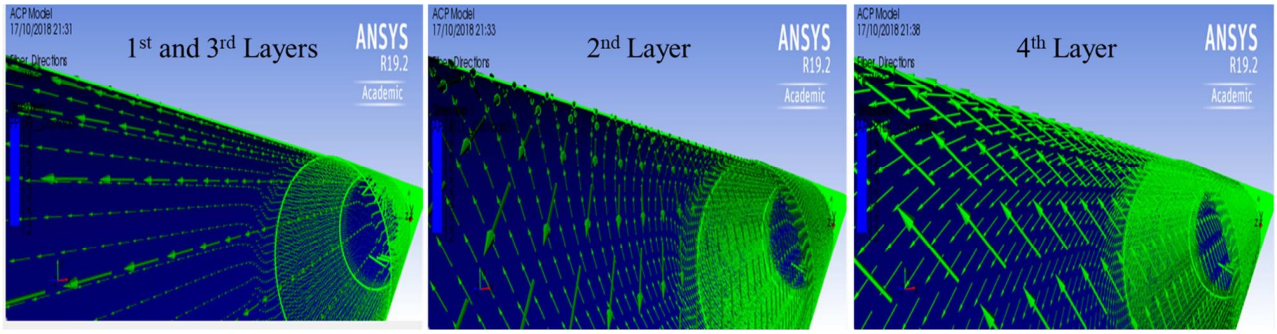

Figure 10. Directions of the fibers modeled for each layer during FEM simulation.

The wing spar model developed in the ANSYS ACP Pre was then exported to the Static Structural simulation module, where the lift loads and the wing spar supports (fixed support) were applied, according to Fig. 11.

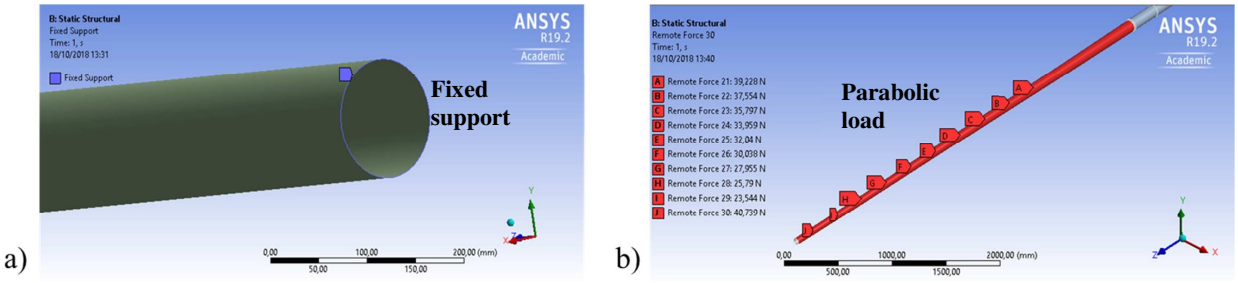

Figure 11. Wing spar simulation: a) Support indication; b) lift load distribution.

After the forces were applied, the simulation was performed and the spar deflection can be seen in Fig. 12.

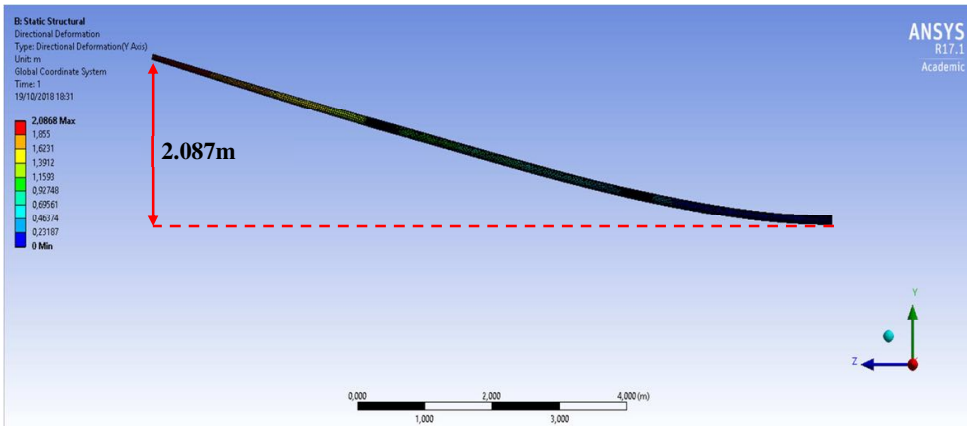

Figure 12. Wing spar vertical deflection – Version 3.

The result showed that the mass of the structre was then below the limit, 4.8kg, but a vertical deflection of 2.087m was reached at the wing spar tip, whose value were above the limit of 600mm. It was then decided to place a Kevlar auxiliary cable that fixed the wing spar to a holder, limiting the deformation of the wing spar through the cable tension. To minimize the tensile stress on the cable and the aerodynamic drag caused by it, the cable support was fixed at the connection between sections 2 and 3 of the wing spar.

Next, a tensile force of 2,750N applyed in the auxiliary cable limiting the deformation was simulated and the result was a vertical deflection of 588mm at the wing spar tip. The mechanical strength of the cable fixing bracket was also verified, according to Fig. 13, obtaining a maximum von Mises stress of 186MPa, and safety factor of 3.2, considered adequate for this project.

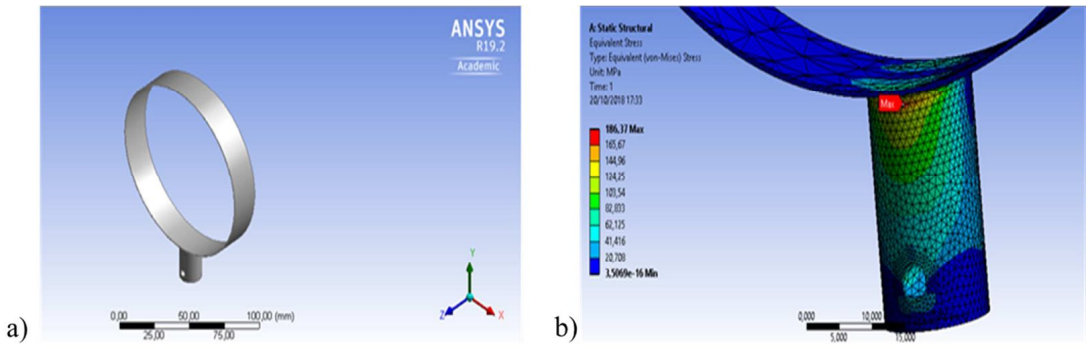

Figure 13. Wing spar simulation: a) Auxiliary cable support geometry. b) Stress distribution.

The maximum stresses of the 4 layers modeled were obtained in this new configuration with the auxiliary cable, including the fiber directions. The first layer main stress direction is represented in Fig. 14(a). The safety coefficient distribuition along the spar was also calculated and its values remained within the limits imposed on the project. Moreover, through the ANSYS ACP Post analysis was possible to perform a failure analysis by the Tsai-Wu failure criterion (Tsai and Wu, 1972 and Hansen, 1992), individually for each layer, in order to garantee the wing spar

structural integrity. The Tsai – Wu failure criteria result of the first layer is represented in Fig. 14(b) reaching maximum valid factor of 0,125.

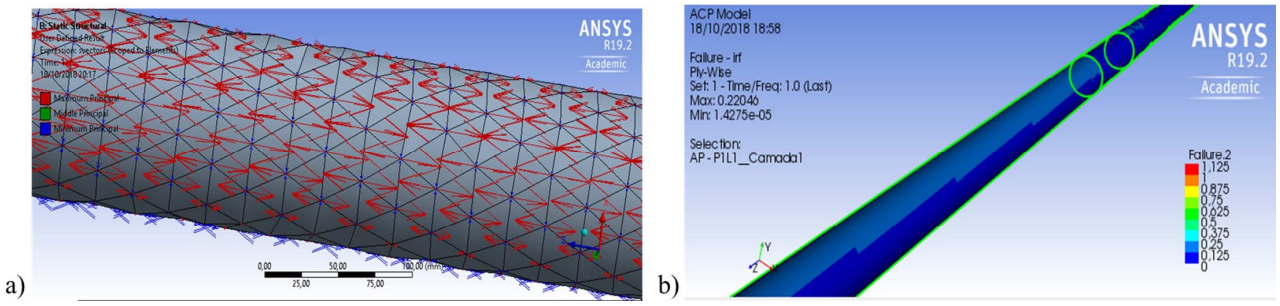

Figure 14. Wing spar simulation: a) Main stress directions (1st layer) b) Tsai – Wu failure criteria result (1st layer).

2.4 Prototype manufacturing

Once the mass, vertical deflection and stress criteria were reached during the numerical simulation stage, two prototypes representing the section 1 of Version 3 were manufactured for experimental validation. The first prototype had Ø115mm x 900mm of dimension and was used for the ribs assembly on the wing spar validation. Already the second prototype had Ø115mm x 1800mm of dimension and aimed to experimentally validate the numerical simulations trough stress analysis.

Both prototypes were manufactured through the lamination process with an constant external diameter of 115mm and a thickness of 1.2mm, composed by four layers of carbon fiber with 0.3mm each. The resin chosen was Araldite 5052 because it is an aeronautical resin with mechanical properties similar to the ones used in the numerical simulations.

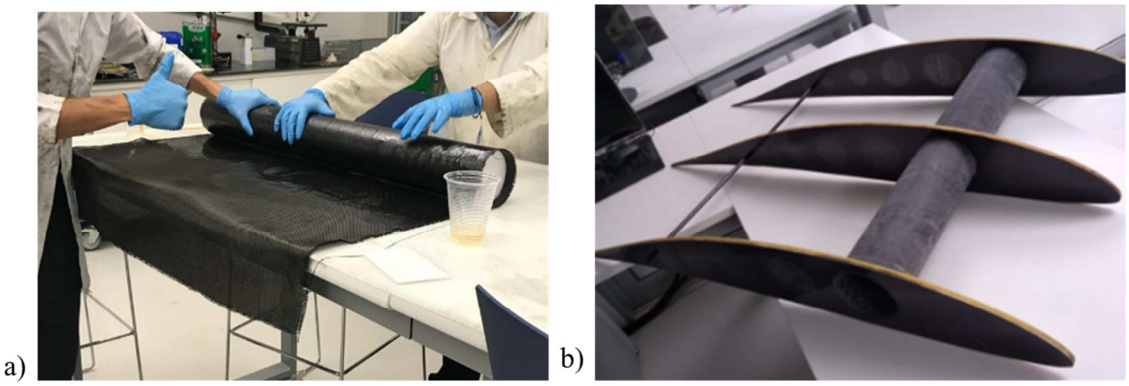

Figure 15. a) Lamination process b) Wing spar assembled with the ribs.

The spar manufacturing consisted in 4 steps. First a polystyrene mold was made, so it could be involved by the carbon fabric impregnated with epoxy, while the rein was being applied (Fig. 15a). Then for the cold curing process, the spar with the fabric and resin was involved in a vacuum bag and with a vacuum bomb the air was drawn. This process aim is to make a uniform resin layer along the spar, avoiding bubbles and consequently increasing the material mechanical properties in 30%-50% in relation to the process without the vacuum bag.

To conclude the wing spar manufacturing, the spar was unmolded and the assembly of ribs on the wing spar was validated as in Fig. 15(b) and then the experimental validation could be done.

2.5 Experimental validation

In this this section, we aimed to compare the results obtained through finite element simulation with the experimental results. In order to do so, the second prototype was assembled on a support in order to evaluate the strength of the wing spar in its first section, called Section 1.

In order to validate the prototype of the wing spar, it had its end fixed in the base support, that simulate the center of the wing and then 5 loads of 7.1kg each spaced of 340mm were also applied according to the boundary conditions used during the numerical simulations.

The criterion considered for the experimental validation was its principal strain measured through an electric strain gage glued on the prototype surface at 285mm position, counting from the fixed base. A schematic of the test can be seen in Fig. 16, as well as a picture of the test. The strain measured through the strain indicator was 522μd.

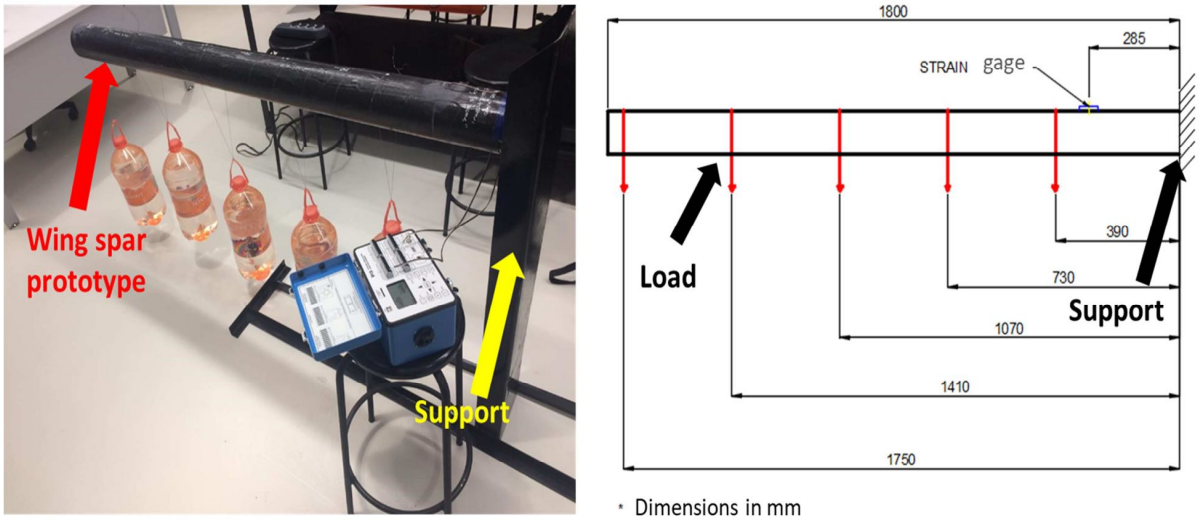

(a) (b)

Figure 16. (a) Prototype loading apparatus. (b) Schematics of the tests.

For numerical validation of the results, a model of this test was performed in ANSYS, with the same dimensions and the same loads applied experimentally. After performing the simulation, it was obtained that the strain at the same point where the strain gage was placed in the prototype was 484μd according to Fig. 17.

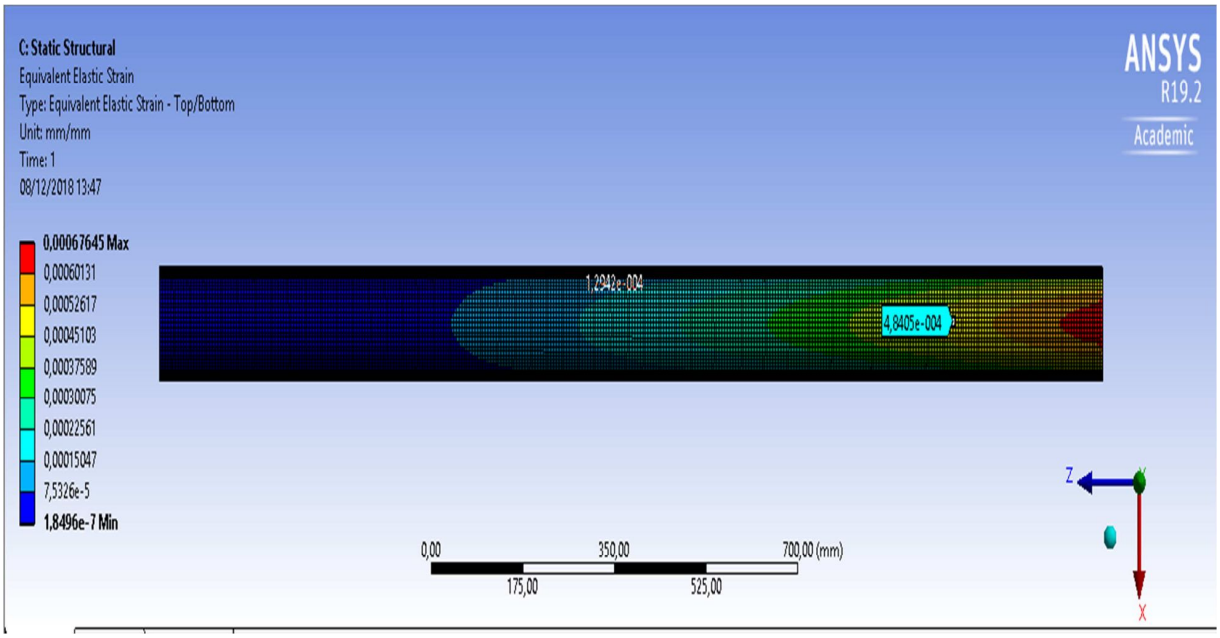

Figure 17. Experiment simulation result.

Thus, an error of 7.28% was obtained, which represents an acceptable error, indicating that the simulation corresponds to the reality with a good level of confidence, thus validating the numerical model developed in this work.

3. CONCLUSIONS

The main conclusions obtained after the end of this research work were:

- Defined dimensions for the wing spar in Version 3 were adequate in both the aerodynamic aspect and structural strength and stiffness.
- According to the numerical simulations carried out, the wing spar structure model reached a maximum deflection of 588mm and a total mass of 4.8kg, meeting all the contour conditions of the project.
- The selected material Epoxy composite + 79% - T800 proved to be suitable for manufacturing the wing spar with good performance both in the manufacturing stage and in the mechanical tests.
- The principal strain result obtained through strain gage measurement was 522μd while the numerical simulation result was 484μd, obtaining a relative error of 7.28%, errors associated with manufacturing process limitations.
- In general, the results indicated that the simulation corresponds to the reality with a good level of confidence, thus validating the numerical model developed in this work, which makes the wing structure feasible to be manufactured for real flight tests in future.

4. ACKNOWLEDGEMENTS

The authors would like to acknowledge Instituto Mauá de Tecnologia (IMT) and ESSS ANSYS for the technical and financial support during this research work.

5. REFERENCES

Anderson Jr., J. D. (1999). *Aircraft performance and design.* Boston: McGraw-Hill.

Ashby, M. F., 2010. *Materials selection in mechanical design*. 5ª. Ed. Butterworth Heinemann. 640pp. ISBN 978-185.617.663-7

Burke, J. D. (1980). *The Gossamer Condor and Albatross: A Case of Study in Aircraft Design.* Pasadena: AeroVironment Inc.

Drela, M., & Giles, M. B. (1987, October). Viscous-Inviscid Analysis of Transonic and Low Reynolds Number Airfoil. *AIAA Journal V25 (10)*, pp. 1347-1355.

Hansen, W. C., 1992. "The significance and measurement of the tsai-wu normal interaction parameter F12". Thesis submitted to Oregon State University. Master of Science – Dept. Mech. Engineering. 105pp.

Niu, M. C. Y., 2001. *Airframe stress analysis and sizing*. 3a Ed. Conmilit Press Ltd. 795pp. ISBN 962-7128.08-2

Royal Aeronautical Society. (2017). Acessed June 23rd, 2017, available at Royal Aeronautical Society: https://www.aerosociety.com/get-involved/specialist-groups/business-general-aviation/human-powered-flight/

Sóbester, A.; Forrester, J.A., 2015. *Aircraft Aerodynamic Design: Geometry and Optimization*. Southamptom: Wiley, Ltd. 246pp. Print ISBN: 978-047.066.257-1

Tsai, S. W.; Wu, E. M., 1972. "Optimal experimental measurements of anisotropic failure tensors". Journal of composite materials". Online ISSN: 1530-793X. DOI 10.1177.

Torenbeek, E. (2013). *Advanced Aircraft Desgin* . Sussex: Wiley and Sons.

Vanderhoydonck, B.; et al., 2016. "Optimization of a human-powered aircraft using fluid-structure interaction simulations". Aerospace MDPI, 2016, 3, 26. DOI: 10.3390.

6. RESPONSIBILITY NOTICE

The authors are the only responsible for the printed material included in this paper.